Indonesian Physical Review
Volume 6 Issue 3, September 2023
P-ISSN: 2615-1278, E-ISSN: 2614-7904

Structure And Morphology Analysis Of Annealing Post-Treatment Thin Film Titanium And Copper-Doped Zinc Oxide

Budi Astuti[1*], Niswatul Abidah[1], Egy Awalia Fatiha[1], Krisna Ardi Nugraha[1]
[1]*Department of Physics, Faculty of Mathematics and Natural Sciences, Universitas Negeri Semarang*

Corresponding Authors E-mail: b_astuti79@mail.unnes.ac.id

Article Info

Article info:
Received: 27-03-2023
Revised: 30-06-2023
Accepted: 08-08-2023

Keywords:
Thin film; Annealing temperature; Spin coating; Ti-Cu doped ZnO

How To Cite:
B. Astuti, N. Abidah, E. A. Fatiha, and K. A. Nugraha "Structure and Morphology Analysis Of Annealing Post-Treatment Thin Film Titanium And Copper Doped Zinc Oxide," Indonesian Physical Review, vol. 6, no. 3, p 334-345, 2023.

DOI:
https://doi.org/10.29303/ipr.v6i3.235

Abstract

Ti-Cu doped ZnO thin film has been successfully deposited on a preparate glass substrate using the spin coating method with post-treatment annealing temperatures of 350°C - 550°C. This research analyzes the structure and morphology of Ti-Cu doped ZnO thin films on DSSC performance. The crystal structure of Ti-Cu doped ZnO thin film was characterized using X-Ray diffraction (XRD) to determine the effect of annealing temperature on the quality of its crystal structure. XRD results show that the crystal structure is dominant in the (101) plane, with lattice parameters in the crystal tending to be constant at a = b = 5.21 and c = 3.25 so that the crystal volume tends to be constant at 47.77 Å. Furthermore, the FWHM value tends to decrease from 0.4419° to 0.2523°, crystal size tends to increase from 19.76 nm to 34.60 nm, dislocation density decreases from 0.0025 nm^{-2} to 0.0008 nm^{-2}, stress decreases from 0.58% to 0.33%, and strain tends to increase from -1.364 GPa to -0.782 GPa. This indicates an improvement in crystal structure along with the addition of an annealing temperature of 350°C - 550°C. The SEM results showed that an annealing temperature of 450°C is a good temperature compared to other film variations, as evidenced by the agglomeration's narrowing and the grain size decrease.

Introduction

Thin films have been widely applied in the industrial sector, among others, such as transistors [1], dye-sensitized solar cell [2], windows layer [3], sensors [4], display devices [5], TCO (Transparent Conducting Oxide) [6], and photoanodes [7]. Dye-sensitized solar cell (DSSC) has four main components: conducting glass substrate, photoanode, counter electrode, and electrolyte [8]. The semiconductor material used as the base material of DSSC must have high chemical stability, morphology structure with good homogeneity, and high electron mobility [9].

Researchers generally use semiconductor materials as hosts, such as Mn_3O_4 [10], SnO_2 [11], TiO_2 [12], VO_2 [13], and ZnO (Astuti et al., 2021). Semiconductor material ZnO is widely chosen as a host or buffer for thin film layers because ZnO has a wide band gap energy (3.37 eV), higher electron mobility than TiO_2 ($115 - 155\ cm^2V^{-1}s^{-1}$), a large enough excitation energy of 60 meV, stable against photo corrosion, cheap and easily available [15], [16]. This indicates that ZnO is suitable for DSSC. However, pure ZnO thin films still have the potential to experience conductance changes caused by oxygen adsorption and chemisorption [17]. Therefore, it is necessary to dope the ZnO thin film layer to overcome this issue.

Some metals that can be doped with ZnO are Fe [18], Al [19], Mg (Astuti et al., 2021), Cu [20], Ti [21]. When ZnO is doped with Ti-Cu, the thin film increases absorbance, has a high refractive index (2.09), and has a smaller band gap energy than pure ZnO thin film [22]. However, few studies have identified the structure and morphology properties of Ti-Cu doped ZnO thin film with varying annealing temperatures. Annealing temperature variation can significantly affect the crystal structure and morphology of DSSC. Annealing temperature variation can increase the diffraction peak and better crystallinity quality of the film at higher annealing temperatures [23], [24] show that the optimum annealing temperature can improve the quality of the crystal structure. In addition, varying the annealing temperature can affect the size and distribution of photosensitive particles, affecting the efficiency of light absorption and electron transfer [25]. Increasing the annealing temperature can cause changes in the crystal structure of the thin film. The atoms can obtain enough energy to move and reach a more stable position, reducing crystal defects and increasing the crystal order in the thin film [26].

The growth of Ti-Cu doped ZnO thin film can be grown through several methods, such as sol-gel spin coating [27], spray pyrolysis [28], hydrothermal [29], and sputtering [30]. The sol-gel spin coating method is a method that utilizes sol-gel (precursor solution) to coat the substrate surface with a fast deposition process, a thickness that can be controlled by adjusting the speed of the centrifugal spinner, more even distribution of material on the substrate surface, controllable film composition, high homogeneity, reproducibility, and low production costs [31], [32].

The obtained Ti-Cu doped ZnO thin films can bed characterized by several techniques. Some characterization techniques are UV-Vis light measurement, electron microscope, and X-Ray. X-Ray measurements are important because these techniques are used to determine the characteristics of thin film materials by identifying the crystal phases of a material [33]. One is the X-Ray measurements, namely X-Ray Diffraction (XRD). XRD measurements are important for Ti-Cu doped ZnO thin film to determine the crystal phases, crystal plane, crystal size, crystal orientation, and crystal quality obtained [34]. The sample characterization results obtained are based on crystallinity, such as JCPS, to ensure the suitability of the sample to be achieved.

Based on the above description, this study synthesizes and characterizes the Ti-Cu doped ZnO thin film layer as a Dye-Sensitized Solar Cell (DSSC) application. The Ti-Cu doped ZnO thin film layer has been deposited and annealed with different annealing temperatures to improve

the quality of the thin film crystal structure based on XRD characterization results such as lattice parameters crystal structure based on hexagonal systems, dislocation lines, strains, and stress.

Theory and Calculation

A thin film is a thin semiconductor material layer that measures nanometers to no more than 10 µm [35]. Thin film coating on solar cells is made based on oxide semiconductors, such as ZnO, TiO_2, and CuO. TiO_2 and CuO double-doped ZnO thin films have previously been grown by Mehmood et al. (2021) with post-treatment variations in CuO concentration (0%; 0.5%; 1%; 1.5%) using the dip coating method. The results showed that TiO_2 and CuO-doped ZnO thin films have a hexagonal wurtzite crystal structure. The structure of the thin film can be calculated using the XRD test results and analyzed, which are then used to determine peak intensity, 2θ peak location, texture coefficient (TC), lattice parameters (a = b, c), volume (V), FWHM, crystallite size (D), grain size (δ), strain (ε), and stress (σ).

TC calculation determines the most dominant crystal plane among other crystal planes. The dominant crystal plane has a TC value > 1. TC can be determined by equation (1).

$$TC = \frac{\frac{I(hkl)}{I0(hkl)}}{\frac{1}{n}\sum\frac{I(hkl)}{I0(hkl)}} \quad (1)$$

TC represents the texture of the coefficient, $I(hkl)$ is the intensity of XRD measurement, $I_0(hkl)$ is the reference intensity of X-ray scattering, and n is the number of reflections of the XRD diffraction pattern. Based on TC calculations, the dominant structure of the thin film can be known, which will then become the focus of discussion to determine lattice parameters, volume, and others. Lattice constants parameters of Ti-Cu doped ZnO are calculated by equation (2)

$$\frac{1}{d^2} = \frac{4}{3}\left(\frac{(h^2+hk+k)}{a^2}\right) + \frac{I^2}{c^2} \quad (2)$$

Here (h, k, l) are Miller indices, and "d" is d-spacing and of hexagonal structure. The obtained lattice parameter values are used to determine the hexagonal structure unit cell volume with equation (3).

$$V = 0{,}868\ x\ a^2\ x\ c \quad (3)$$

With V being the unit cell volume of the hexagonal structure, a = b and c being the lattice parameters of the hexagonal structure. The quality of the crystal structure can further be identified from the crystallite size using Scherrer's equation (4).

$$D = \frac{0.9\lambda}{\beta coscos\ \theta} \quad (4)$$

With D as the crystallite size, λ as the X-ray wavelength (λ = 0.15046 nm, θ as the diffraction angle, and β as the FWHM (Full Width at Half Maximum). The results of the crystallite size calculation can determine the magnitude of the dislocation line as shown in the equation (5).

$$\delta = 1/D^2 \quad (5)$$

Where δ is the dislocation density and D is the crystal size. Equation (5) shows that the dislocation density is inversely proportional to the crystal size. Furthermore, The quality of the crystal structure can then be known by the strain value on the crystal. The strain value can be known using the Calculation of equation (6).

$$\beta = 4\varepsilon \, tan\theta \quad (6)$$

where β is the FWHM value, ε is the amount of strain on the crystal structure, and θ is the diffraction angle (hkl). The strain value obtained is used to determine the stress value with the formula equation (7) [27].

$$\sigma = -233 \, \varepsilon \quad (7)$$

Where σ is the stress value on the thin film and ε is the magnitude of the strain on the crystal structure. The small value of strain indicates crystals that are not easily dislocated.

Experimental Method

Materials prepared as Ti-Cu double-doped ZnO precursors were Zinc acetate dehydrate (Merck, 99.5%), Copper (II) acetate monohydrate (Merck, 99.5%), Thiourea (Loba Chemie, 99%). The solvent used 2-Propanol (Merck, 99.8%) and monoethanolamine (99%). The substrate used preparate glass (Sail Brand) cut into 1 cm x 1 cm size, washed using methanol and acetone in an ultrasonic bath for 15 minutes, and dried using nitrogen. Sol solution was prepared by dissolving 1.632 grams of zinc acetate dehydrate ($Zn(CH_3COO)2.2H_2O$) into isopropanol solvent (15 mL), then stirred using a magnetic stirrer at 60°C for 15 minutes. In the same way, add 1% copper (II) acetate monohydrate ($Cu(CH_3COO)2.H_2O$) (0.0149 gram). Once homogenized, add 1% titanium oxide (TiO_2) and stir for 60 minutes. The homogeneous solution was added to ethanolamine stabilizer and stirred for 60 minutes. Next, the solution was allowed to stand for 24 hours at room temperature for the aging process. Ti-Cu doped ZnO precursor solution (0.01 mL) was deposited on a substrate previously heated on a hot plate at 120^o C for 10 minutes. The Ti-Cu doped ZnO thin film was grown using the sol-gel spin coating method at 3.400 rpm for 15 seconds. Next, the Ti-Cu doped ZnO thin film was annealed with a preheating temperature of 300^o C for 15 minutes. Preheating aims to evaporate solvents and organic components in the thin film. To get a good thin film, then holding for 120 minutes in the annealing process for temperature variations of 350^o C, 400^o C, 450^o C, 500^o C, and 550^o C. Ti-Cu doped ZnO thin films obtained, characterized using X-Ray diffraction (XRD) from D8 Advanced.

Result and Discussion

Structure

The crystal structure of Ti-Cu doped ZnO thin films has been obtained from XRD characterization displayed in Figure 1. The results of XRD analysis show data on texture coefficient (TC), lattice parameters (a = b, c), volume (V), FWHM, crystallite size (D), grain size (δ), strain (ε), and stress (σ). The diffraction peaks of Ti-Cu doped ZnO thin film are dominant at three diffraction peaks, namely 2θ = 31.8; 34.5; and 36.4 corresponding to planes (100), (002),

and (101), respectively. In addition, other diffraction peaks are visible in Figure 1, namely (110) and (013). The diffraction peak (110) with 2θ = 56.9 for an annealing temperature variation of 350°C and 2θ = 56.7 for an annealing temperature variation of 550 °C, while the diffraction peak (013) at 2θ = 63.0 with annealing temperature variation of 550 °C. The data obtained confirms that the crystal structure of Ti-Cu doped ZnO thin film is hexagonal wurtzite polycrystal type and is following JCPDS No.96-901-1663 [36].

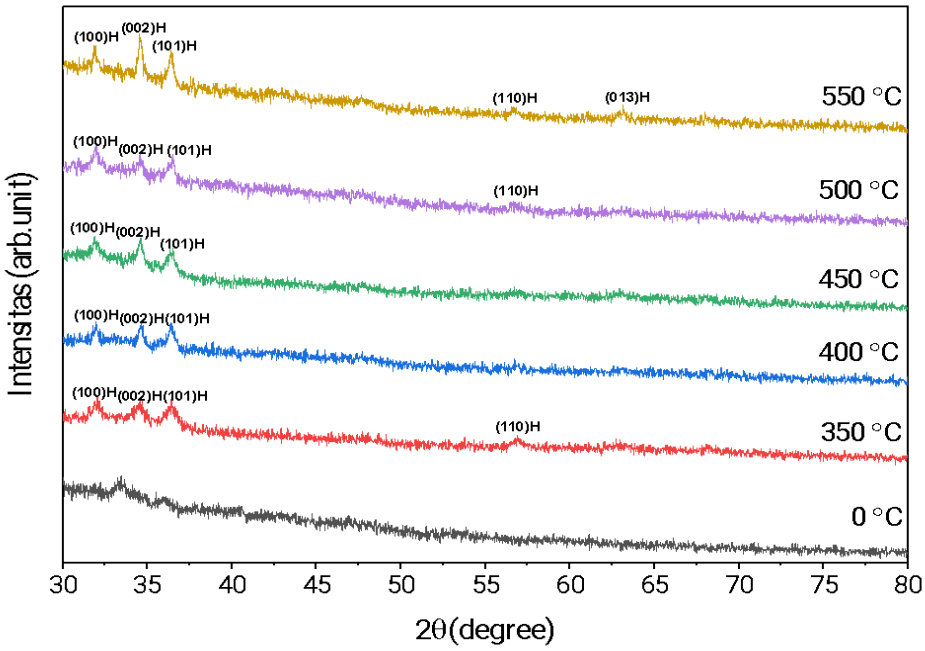

Figure 1 Spectrum analysis XRD Ti-Cu doped ZnO thin film.

Based on Figure 1. shows the diffraction peaks of the crystal planes (001), (002), and (101) have almost uniform intensity. This is due to the thickness of the film, which is quite thin. Therefore, it is necessary to calculate the texture coefficient (TC). The TC calculation results are shown in Table 1. Shows that the crystal plane structure (101) has a TC value > 1 for all annealing temperature variations. This is because the (101) crystal plane structure is required for DSSC applications. For further discussion will be focused on the crystal plane (101).

The quality of the characteristics structure is can be known from lattice parameters ($a = b, c$). The values of lattice parameters a, b, and c in the crystal structure didn't change the structure of the crystal plane. This can be seen in Table 2. which shows that the lattice parameter values have fixed values at all annealing temperature variations, which are around $a = b = 5.21$ Å and $c = 3.25$ Å. The constant lattice parameter values indicate the incorporation of Ti and Cu into the ZnO lattice does not produce a new phase. The lattice parameter values of Ti-Cu doped ZnO thin films follow JCPDS No.36-1451 [36]. The constant lattice parameters indicate that the interatomic distance and bond angle are constant so that they can cause a change in DSSC efficiency.

Table 1. Structure and lattice parameters of Ti-Cu doped ZnO thin films with varying annealing temperatures (350° C-550° C)

T(°C)	hkl		
	100	**002**	**101**
0	0	0.2182	0
350	0.9993	0.7903	1.2103
400	1.1182	1.0615	1.2103
450	0.9993	0.7903	1.2103
500	1.1182	1.0615	1.2103
550	0.9993	0.7903	1.2103

This is because the crystal structure, electrical conductivity, and electron transfer efficiency of the thin film can be affected by changes in temperature. As the temperature increases, the atoms in the thin layer oscillate faster, altering the crystal structure. As a result, efficiency varies with temperature while lattice parameters remain constant [37]. Besides the lattice parameter, the unit cell volume obtained also has a value that tends to be constant at all annealing temperature variations of 47.77 $Å^3$. This shows that the annealing temperature does not affect the volume of the crystal plane structure.

Table 2. Resume of structure and lattice parameters Ti-Cu doped ZnO thin film with various annealing temperatures annealing (350 °C-550 °C)

	350 °C	400 °C	450 °C	500 °C	550 °C
a = b, c (Å)	a = b = 5,21 c = 3,25	a = b = 5,21 c = 3,25	a = b = 5,21 c = 3,25	a = b = 5,21 c = 3,25	a = b = 5,21 c = 3,25
V (Å)^3	47,77	47,77	47,77	47,77	47,77
FWHM (°)	0,4419	0,2232	0,2838	0,2664	0,2523
D (nm)	19,76	39,12	30,77	32,78	34,60
δ (nm^{-2})	0,0025	0,0006	0,001	0,0009	0,0008
ε (%)	0,58	0,29	0,37	0,35	0,33
σ (GPa)	-1,364	-0,690	-0,878	-0,823	-0,782

Table 2. also shows that the FWHM value is affected by the different annealing temperatures. The addition of annealing temperature resulted in the thin film tending to narrow the FWHM from 1.7187° to 0.7077°. The smaller FWHM value indicates better crystal quality because the smaller the FWHM; the easier it is for the atoms to set the bond length and direction [38]. The FWHM value is inversely proportional to the crystal size. The smaller the FWHM value, the larger the crystal size, which means the higher the DSSC efficiency, and otherwise. it is shown in Figure 2.

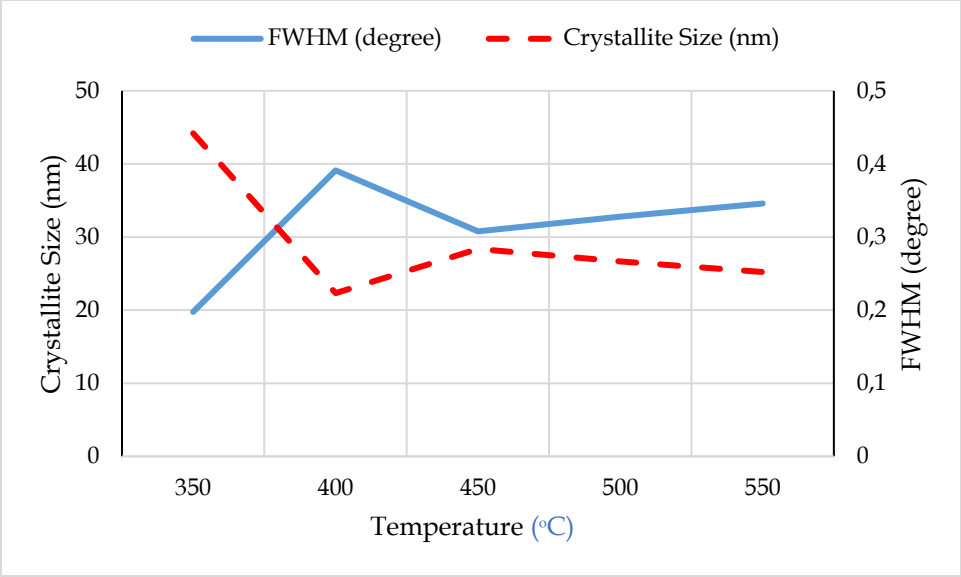

Figure 2. Relationship between FWHM value and crystallite size

The crystal size obtained at each annealing temperature variation is 29.76 nm; 39.12 nm; 30.77 nm; 32.78 nm; and 34.60 nm. The increase was quite drastic at 400°C, which was influenced by the decrease in FWHM value. The decrease in FWHM value may occur due to strains. Strain can occur due to differences in the radius of Zn^{2+} ions (r = 0.074 nm), the radius of Ti^{4+} ions (r = 0.068 nm), and the radius of Cu^{2+} ions (r = 0.096 nm) [39], [40]. After that, the crystal size decreased when the temperature was 450°C. The smaller crystal size can increase the light absorption efficiency because it increases the contact surface area with the electrolyte.

The quality of characteristics of thin film structure further on dislocation line. Dislocation line density is inversely proportional to the crystal size. The larger the crystal size, the smaller the dislocation density. A large dislocation density indicates many defects in the crystal structure, causing lattice distortion, while a small dislocation density indicates an improved crystal structure. A high dislocation density indicates many defects in the crystal structure, leading to lattice distortion, while a low dislocation density indicates a better crystal structure. High dislocation density can lead to higher electron-hole recombination and reduce energy conversion efficiency. [41]. Table 2 shows a decrease in dislocation density in the sample from 0.0025 nm^{-2} to 0.0008 nm^{-2}. This means that the Ti-Cu doped ZnO thin film has an improved crystal structure and the addition of annealing temperature. The decrease in dislocation line density in the crystal structure occurs due to the addition of annealing temperature giving more space for atoms, so they can shift and shift to form perfect crystals [42].

Furthermore, the quality of the crystal structure can then be known by the strain value on the crystal. The small value of strain indicates crystals that are not easily dislocated, while the small value of stress indicates the weak binding force of the atoms that make up the crystal. It is known that the addition of annealing temperature increases stress value. It can be assumed that the addition of annealing temperature triggers the strength of the binding force between atoms so that the arrangement of the atomic configuration becomes more stable.

Morphology

SEM images of ZnO doped Ti-Cu with post-treatment annealing 0 ^{o}C, 350 ^{o}C, 400 ^{o}C, 450 ^{o}C, 500 ^{o}C, 550 ^{o}C are shown in Figure 3a to Figure 3f.

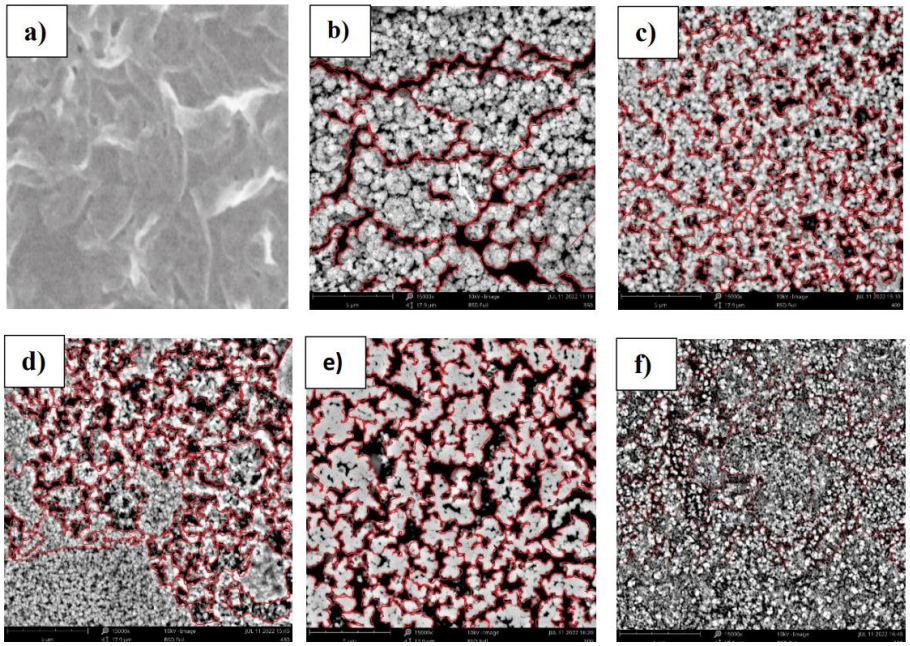

Figure 3. Morphology of Ti-Cu double-doped ZnO thin films with varying annealing a.) 0 ^{o}C, b.) 350 ^{o}C, c.) 400 ^{o}C, d.) 450 ^{o}C, e.) 500 ^{o}C, e.) 550 ^{o}C at 15,000 times magnification

Figure 3a. The pure ZnO thin film sample without annealing shows a cloudy surface [43]. Furthermore, the surface is cloudy after the ZnO thin film is doped with Ti-Cu and post-treated. After doping the ZnO thin film with Ti-Cu and post-treating with different annealing temperatures, the surface of the thin film is granular. The granular shape is a of grain and crystal growth [44]. When the thin film is subjected to different annealing temperature treatments, the atoms in the sample have enough energy to vibrate. have enough energy to vibrate to occupy a more stable position. The addition of annealing temperature results in heat vibrational energy, affecting the speed of atomic fusion to cross grain boundaries and join between grains into large structures. Figure 3b. to Figure 3f. also shows the agglomeration or clumping of the thin film surface morphology, such as the thin film surface's sample size and grain size, which becomes narrower as the annealing temperature increases. Agglomeration is a condition where small grains combine to form larger structures due to an increase in physical properties such as temperature.

Furthermore, Figure 3b to Figure 3f also confirms the XRD data that the 450^{o}C annealing temperature is a thin film layer with uniformity. It is the thin film layer with the most optimal uniformity among the other thin film samples. This is evidenced by the appearance of agglomerated grains in Figure 3a to Figure 3b. The figure shows that when the sample is annealed at a temperature of 350^{o}C, the sample experiences a large amount of agglomeration. Then, after increasing the annealing temperature (400 ^{o}C-450 ^{o}C), the agglomeration narrowed. It widened when the sample was annealed at a temperature of 500^{o}C.

Conclusion

The spin coating method deposited ti-Cu doped ZnO thin films on the prepared glass substrate. This study aims to determine the effect of annealing temperature on the structure and morphology of Ti-Cu doped ZnO thin films. XRD analysis results show that all annealing temperature variations have a hexagonal wurtzite-shaped crystal structure with an increase in crystal size, a decrease in dislocation density, a decrease in strain, and an increase in stress in the crystal structure of Ti-Cu doped ZnO thin films with increasing annealing temperature. Meanwhile, the SEM results show a change in the surface morphology characterized by a change in the surface shape from cloudy to granular and a change in the degree of agglomeration with the addition of annealing temperature, as for the agglomeration narrowing when the annealing temperature is 450^{o}C.

References

[1] Y. Kuo, "Thin film transistor technology-Past, present, and future," *Electrochem. Soc. Interface*, vol. 22, no. 1, pp. 55–61, 2013, doi: 10.1149/2.F06131if.

[2] Hardeli, Suwardani, Riky, F. T, Maulidis, and S. Ridwan, "Dye Sensitized Solar Cells (DSSC) Berbasis Nanopori TiO2 Menggunakan Antosianin dari Berbagai Sumber Alami," in *Semirata FMIPA Universitas Lampung*, 2013, pp. 155–162.

[3] B. Astuti, I. Maftuchah, and N. Arina, "Bab Vii . Efek Daya Plasma Terhadap Sifat Fotoluminesen Film Tipis ZnO Doping Al," *Kimia*, no. 1, pp. 160–196, 2021, doi: 10.15294/ik.v1i1.66.

[4] P. Banerjee and A. Lakhtakia, *Thin Film Nanophotonics*, no. August. Amsterdam, 2021.

[5] C. Huo and M. Dai, "Transparent Nano Thin-Film Transistors for Medical Sensors , OLED and Display Applications," *Int. J. Nnaomedicine*, vol. 15, pp. 3597–3603, 2020, doi: 10.2147/IJN.S228940.

[6] Sulhadi *et al.*, "Influence of annealing temperature on the morphology and crystal structure of Ga-doped ZnO thin films Influence of annealing temperature on the morphology and crystal structure of Ga-doped ZnO thin films," in *Journal of Psics Conferencesics Conference*, 2019, vol. 1170, pp. 1–4, doi: 10.1088/1742-6596/1170/1/012066.

[7] F. Babar *et al.*, "Nanostructured photoanode materials and their deposition methods for efficient and economical third generation dye-sensitized solar cells: A comprehensive review," *Renew. Sustain. Energy Rev.*, vol. 129, no. C, p. 109919, 2020, doi: 10.1016/j.rser.2020.109919.

[8] S. N. Karthick, K. V Hemalatha, S. K. Balasingam, F. M. Clinton, and S. Akshaya, "Dye-Sensitized Solar Cells : History , Components , Configuration , and Working Principle," in *Interfacial Engineering in Functional Materials for Dye-Sensitized Solar Cells*, A. Pandikumar, K. Jothivenkatachalam, and K. Bhojanaa, Eds. John Wiley & Sons, Inc, 2020.

[9] N. Jamalullail, I. S. Mohamad, M. N. Norizan, N. Mahmed, and B. Nadia, "Recent improvements on TiO2 and ZnO nanostructure photoanode for dye sensitized solar cells : A brief review," in *EPJ Web of Conferences*, 2017, vol. 162, pp. 1–5, doi:

10.1051/epjconf/201716201045.

[10] O. Bayram, M. Emrah, E. Erdal, I. Harun, and O. Simsek, "Synthesis and characterization of Zn-doped - Mn 3 O 4 thin films using successive ionic layer adsorption and reaction technique : Its structural , optical and wettability properties," *J. Mater. Sci. Mater. Electron.*, vol. 29, no. 11, pp. 9466–9473, 2018, doi: 10.1007/s10854-018-8980-9.

[11] I. M. El Radaf, T. A. Hameed, T. M. Dahy, and G. M. El, "Synthesis, Structural, Linear and Nonlinear optical properties of chromium doped SnO2 thin films," *Ceram. Int.*, vol. 45, no. 3, pp. 1–9, 2018, doi: 10.1016/j.ceramint.2018.10.189.

[12] A. S. Bakri *et al.*, "Effect of annealing temperature of titanium dioxide thin films on structural and electrical properties," in *International Conference on Engineering, Science and Nanotechnology*, 2016, vol. 1788, pp. 1–9, doi: 10.1063/1.4968283.

[13] V. Devthade and S. Lee, "Synthesis of vanadium dioxide thin films and nanostructures Synthesis of vanadium dioxide thin films and nanostructures," *AIP Adv.*, vol. 10, no. August 2020, pp. 1–54, 2021, doi: 10.1063/5.0027690.

[14] B. Astuti, A. Zhafirah, N. Hamid, D. Aryanto, and P. Marwoto, "Structure , morphology , and optical properties of ZnO : Mg thin film prepared by sol-gel spin coating method," *J. Ilm. Pendidik. Fis. A-Biruni*, vol. 10, no. 2, pp. 241–250, 2021, doi: 10.24042/jipfalbiruni.v10i2.7239.

[15] S. Il Cho, H. K. Sung, S. J. Lee, W. H. Kim, D. H. Kim, and Y. S. Han, "Photovoltaic performance of dye-sensitized solar cells containing ZnO microrods," *Nanomaterials*, vol. 9, no. 12, pp. 1–12, 2019, doi: 10.3390/nano9121645.

[16] P. Marwoto, Sugianto, Sulhadi, D. Aryanto, E. Wibowo, and Yanti, "Highly Oriented ZnO:Al Thin Films as an Alternative Transparent Conducting Oxide (TCO) for Windows Layer of Solar Cells," *Adv. Mater. Res.*, vol. 1123, pp. 364–367, 2015, doi: 10.4028/www.scientific.net/amr.1123.364.

[17] R. Vittal and K. C. Ho, "Zinc oxide based dye-sensitized solar cells: A review," *Renew. Sustain. Energy Rev.*, vol. 70, pp. 920–935, 2017, doi: 10.1016/j.rser.2016.11.273.

[18] C. Han, L. Duan, X. Zhao, Z. Hu, Y. Niu, and W. Geng, "Effect of Fe doping on structural and optical properties of ZnO films and nanorods," *J. Alloys Compd.*, 2018, doi: 10.1016/j.jallcom.2018.08.217.

[19] J. Ghosh, R. Ghosh, and P. K. Giri, "Sensors and Actuators B : Chemical Tuning the visible photoluminescence in Al doped ZnO thin film and its application in label-free glucose detection," *Sensors Actuators B. Chem.*, vol. 254, pp. 681–689, 2018, doi: 10.1016/j.snb.2017.07.110.

[20] B. Astuti *et al.*, "X-ray diffraction studies of ZnO : Cu thin films prepared using sol-gel method," in *journal of physics conference*, 2020, pp. 1–7, doi: 10.1088/1742-6596/1567/2/022004.

[21] S. Uyar, B. Coskun, M. İlhan, and M. M. Koc, "Optoelectronic Properties of ZnO:TiO2 Nanocomposite Thin Films," *J. Mater. Electron. Devices*, vol. 5, no. 1, pp. 21–27, 2021, [Online]. Available: http://www.dergi-fytronix.com/index.php/jmed/article/view/140.

[22] B. Mehmood, M. I. Khan, M. Iqbal, A. Mahmood, and W. Al-Masry, "Structural and optical properties of Ti and Cu co-doped ZnO thin films for photovoltaic applications of dye sensitized solar cells," *Int. J. Energy Res.*, vol. 45, no. 2, pp. 2445–2459, 2021, doi: 10.1002/er.5939.

[23] Muaz Akm, H. U, I. Fatimah, T. KL, M. M. S, and L. Wei-Wen, "Effect of annealing temperatures on the morphology, optical and electrical properties of TiO2 thin lms synthesized by the sol–gel method and deposited on Al/TiO2/SiO2/p-Si," *Microsyst Technol*, vol. 22, no. 4, pp. 871–881, 2016, doi: https://doi.org/10.100/s00542-015-2514-7.

[24] U. Chaitra, D. Kekuda, and K. Mohan Rao, "Effect of annealing temperature on the evolution of structural, microstructural, and optical properties of spin coated ZnO thin films," *Ceram. Int.*, vol. 43, no. 9, pp. 7115–7122, 2017, doi: 10.1016/j.ceramint.2017.02.144.

[25] D. K. Muthee and B. F. Dejene, "Effect of annealing temperature on structural, optical, and photocatalytic properties of titanium dioxide nanoparticles," *heliyon*, vol. 7, no. 6, 2021, doi: https://doi.org/ 10.1016/j.heliyon.2021.e07269.

[26] H. Cai, K. Tuokedaerhan, L. Zhenchuan, R. Zhang, and H. Du, "Effect of Annealing Temperature on the Structural, Optical, and Electrical Properties of Al-Doped ZrO2 Gate Dielectric Films Treated by the Sol–Gel Method," *Coatings*, vol. 12, p. 1873, 2022, doi: https://doi.org/10.3390/ coatings12121837.

[27] D. Aryanto, "Preparation and structural characterization of ZnO thin films by sol-gel method," in *journal of physics conference*, 2017, pp. 1–9, doi: 10.1088/1742-6596/817/1/012025.

[28] R. B. Rajput, R. Shaikh, J. Sawant, and R. B. Kale, "Recent developments in ZnO-based heterostructures as photoelectrocatalysts for wastewater treatment : A review," *Environ. Adv.*, vol. 9, p. 100264, 2022, doi: 10.1016/j.envadv.2022.100264.

[29] H. Zhang, Y. Lv, C. Yang, and H. Chen, "One-Step Hydrothermal Fabrication of TiO 2 / Reduced Graphene Oxide for High-Efficiency Dye-Sensitized Solar Cells," *J. Electron. Mater.*, vol. 47, no. 2, pp. 1630–1637, 2018, doi: 10.1007/s11664-017-5973-z.

[30] A. Roy and A. Majumdar, "Optoelectronic and surface properties of CuO clusters: thin film solar cell," *J. Mater. Sci. Mater. Electron.*, vol. 32, no. 23, pp. 27823–27836, 2021, doi: 10.1007/s10854-021-07165-x.

[31] C. Rameshkumar, D. Ananth, V. Divyalakshmi, M. Balakrishnan, G. Senthilkumar, and R. Subalakshmi, "An Investigation of SnO2 Nanofilm for Solar Cell Application By Spin Coating Technique," in *AIP Conference Proceedings*, 2021, vol. 2341, doi: 10.1063/5.0050617.

[32] X. Wu, "Preparation of Bi-based photocatalysts in the View Article Online DOI: 10.1039/D0TA01180K Form of Powdered Particles and Thin Films: A Review," *J. Mater. Chem. A*, vol. 8, no. 31, pp. 15302–15318, 2020, doi: 10.1039/D0TA01180K.

[33] R. Dowais, S. Al Sharie, M. Araydah, S. Al Khasawneh, F. Haddad, and A. AlJaiuossi, "Pearl-white gallstones: A report of a case and a chemical analysis by FTIR and XRD," *Int. J. Surg. Case Rep.*, vol. 87, p. 106449, 2021, doi: 10.1016/j.ijscr.2021.106449.

[34] Z. Sinaga, "Analisis Ukuran Kristal Dan Sifat Magnetik Melalui Proses Pemesinan Milling Menggunakan Metode Karakterisasi Xrd , Mechannical Alloying , Dan Ultrasonik Tekanan Tinggi Pada Material Barium Hexaferrite (Bafe12o19)," *J. Kaji. Tek. Mesin*, vol. 5, no. 1, pp. 9–14, 2020.

[35] W. Amananti and H. Sutanto, "Analisis Sifat Optis Lapisan Tipis ZnO , TiO 2 , TiO 2 : ZnO , dengan dan Tanpa Lapisan Penyangga yang Dideposisikan Menggunakan Metode Sol-Gel Spray Coating," *J. Fis. Indones.*, vol. XIX, no. 55, pp. 41–44, 2015.

[36] J. Chauhan, N. Shrivastav, A. Dugaya, and D. Pandey, "Synthesis and characterization of Ni and Cu doped Zno," *J. Nanomedicine Nsnotechnology*, vol. 8, pp. 1–8, 2019, doi: 10.15406/mojps.2017.01.00005.

[37] H. Meddeb *et al.*, "Tunable Photovoltaics: Adapting Solar Cell Technologies to Versatile Applications," *Adv. Energy Mater.*, vol. 12, no. 28, 2022, doi: https://doi.org/10.1002/aenm.202200713.

[38] K. P. M. S. Wahyuningsih, "Konduktivitas dan Transmitansi Film Tipis Zinc Oxide yang Dideposisikan Pada Temperatur Ruang," *Unnes Phys. J.*, vol. 2, no. 1, pp. 37–43, 2013, doi: http://journal.unnes.ac.id/sju/index.php/upj.

[39] M. A. R. Pambudi and S. Suprapto, "Penentuan Kadar Tembaga (Cu) dalam Sampel Batuan Mineral," *J. Sains dan Seni ITS*, vol. 7, no. 2, pp. 20–23, 2019, doi: 10.12962/j23373520.v7i2.30088.

[40] E. Pratiwi, H. Harlia, and A. B. Aritonang, "Sintesis TiO2 terdoping Fe3+ untuk Degradasi Rhodamin B Secara Fotokatalisis dengan Bantuan Sinar Tampak," *Positron*, vol. 10, no. 1, pp. 57–63, 2020, doi: 10.26418/positron.v10i1.37739.

[41] B. D. Siswanto, "Pengaruh Temperatur Artificial Age Terhadap Kekerasan, Kekuatan Luluh dan Kerapatan Dislokasi Pada Paduan Al97,11Mg1,52Si0,86Zn0,51," *J. Mech. Eng. Manuf. Mater. Energy*, vol. 5, no. 2, pp. 115–133, 2021, doi: 10.31289/jmemme.v5i2.4630.

[42] K. W. Böer and U. W. Pohl, "Semiconductors, Optical Materials, Electrical and Electronic Engineering, Applied and Technical Physics, Electronic Devices, Laser," in *Semiconductor Physics*, 2020, p. 1200.

[43] C. H. Burgess, R. Kilmurray, and M. A. Mclachlan, "Effect of processing temperature on fi lm properties of ZnO prepared by the aqueous method and related organic photovoltaics and LEDs," *R. Soc. Chem.*, vol. 7, no. 15, pp. 2809–2817, 2020, doi: 10.1039/d0qi00497a.

[44] C. . Ching, P. . Ooi, Z. Hassan, A. Hassan, and M. Abdullah, "Structural Properties of Zinc Oxide Thin Films Deposited on Various Substrates," *Sains Malaysiana*, vol. 43, no. 6, pp. 923–927, 2014.